Journal of Friction and Wear
Vol. 20, No. 6, pp. 35-44, 1999

Trenie i Iznos
UDC 621.891

ATOMIC FORCE MICROSCOPY OF TiN FRICTION SURFACE

H.S. Ahn, S.A. Chizhik, and A.M. Dubravin

The surface of TiN coating and its changes have been analyzed in the process of sliding friction on steel. The method of atomic force microscopy (AFM) was used in the intermittent mode followed by imaging of the phase contrast. Friction results in the general smoothing of the surface topography. After friction four types of regions were distinguished and visualized on the TiN surface: hard coating material, steel debris accumulating in relief valleys, steel smeared plastically over relief slopes and softest layers of films 2—5 nm thick on tops of asperities. Analysis of the AFM measurements of the contact zone and computer simulation of the results allow us to assert a combined effect of the mechanisms of fatigue, adhesive and chemical wear of the TiN-steel couple. Adhesive wear with steel transfer to the TiN surface may play the most significant role.

Deposition of functional coatings is one of the most effective methods of creating friction surfaces satisfying the needs of modern mechanical engineering. Hardening of contacting surfaces is achieved by applying the surface layers of hard materials, such as ceramic oxides, carbides, and nitrides. Titanium nitride (TiN) coatings possess sufficient hardness, high protective and good technological properties that makes them an attractive tool of promoting the wear resistance of friction units and extending the service life of machining tools. Though the behavior of TiN coatings has always attracted interest [1], their mechanisms of wear in contact with softer materials, for example steels, remain rather unclear. Since TiN coatings demonstrate exceptional wear resistance, highly sensitive techniques of surface analysis are needed to register minor changes of friction surfaces. The techniques of modern atomic force microscopy have been employed to investigate TiN friction surfaces, yielding rather clear understanding of the minutest modifications of surfaces at friction by combining the analysis of the surface topography with that of the non-homogeneity of micromechanical properties of surface layers.

Object of Studies. A disk of hardened steel EN31 was coated with TiN by ion sputtering in vacuum using an electric arc source. The resulting coating was 3 μm thick (Fig. 1) because TiN coatings 2—3 μm thick are reported to provide the most reliable protection of friction surfaces and high fatigue resistance [1]. Thicker coatings yield chip debris which initiate abrasive wear.

Tests were performed by dry rolling friction of a roller from bearing steel (FAG) on the TiN-coated steel disk (Fig. 2). The roller diameter was 6 mm, its length was 5.3 mm. Roughness and micromechanical properties of friction surfaces and the substrate were checked (see the table). A profilometer (Talysurf) served for roughness measurements. The load applied to the roller was P = 80 N, the sliding velocity was v = 1.0 m/s.

Methods of Studies by Atomic Force Microscopy. Friction surfaces were studied using the method of atomic force microscopy (AFM) with the measuring complex NANOTOP-203 designed and fabricated by the Metal-Polymer Research Institute of the Belarus National Academy of Sciences [2].

Recently application of the oscillation probe and new modes of imaging have added significantly to the progress of atomic force microscopy. The intermittent mode employed in the studies served to avoid damage of studied surfaces by contact scanning of soft materials and to promote reliable performance in the non-contact mode. In the intermittent mode the probe oscillates with a frequency

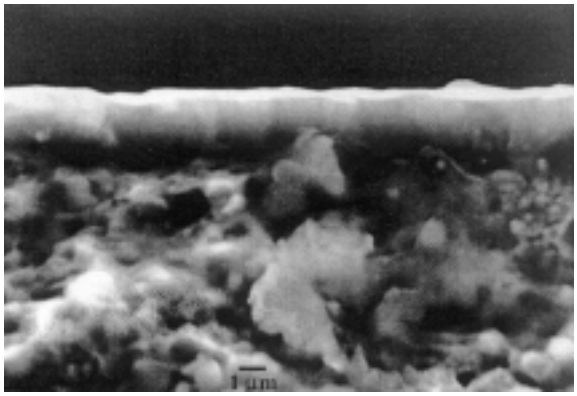

Fig. 1. Electron microscopic image of cross-section of TiN coating on steel

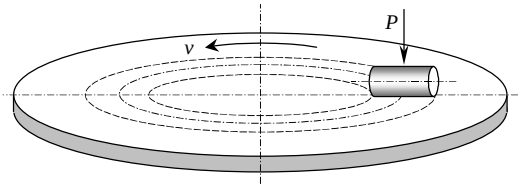

Fig. 2. Schematics of TiN coating friction tests

Table

Roughness and Mechanical Properties of the Specimens

Monitoring parameters	TiN coating	Roller of bearing steel	Hardened steel substrate
Arithmetic average roughness R_a, μm	0.13–0.20	along the cylinder element – 0.1; along the periphery – 0.015	0.05
Young modulus, GPa	400	180	200
Vickers microhardness, HV	710	800–850	860–880

about 100 kHz for imaging the surface and minimizing the non-elastic surface deformation by reducing the duration of contact between the probe and the specimen. However, this mode does not eliminate forces of interactions between the tip and the specimen. During each oscillation cycle the probe tip remains for some time close to the surface of the specimen and directly contacts it, the tip of the probe feels the action of the forces of attraction and repulsion.

When scanning the portions of the surface with different micromechanical properties in the intermittent mode, the phase of oscillations of the probe changes. These variations of the phase are registered in an auxiliary file of images in addition to the file of the Z-position of the tip describing the topography of the test portion of the surface.

It is a rather intricate problem to interpret the test image of the phase contrast. It is essential to investigate how the angles of the phase of oscillations relate to the force of interactions between the probe and the specimen in order to understand the image of AFM intermittent mode phase [3].

Let us consider a freely oscillating cantilever having a constant of rigidity k, mass m, and figure of merit Q [12]. The resonance frequency of oscillations ω_0 relates to k and m as a dependence $k = m\omega_0^2$. The phase angle ϕ of free oscillations of the cantilever can be recorded (in radians) as a function of the frequency of oscillations ω

$$\phi = \tan^{-1}\left[\frac{m\omega\omega_0}{Q\left(k - m\omega^2\right)}\right] . \qquad (1)$$

Depending on ω, the phase angle changes close to ω_0: $\phi = \pi/2$ for $\omega = \omega_0$, less then $\pi/2$ for $\omega < \omega_0$ and $> \pi/2$ for $\omega > \omega_0$. When the oscillating cantilever is brought close to the surface of the specimen the characteristics of oscillations are altered by the interactions between the tip and the specimen. The forces of interactions between them should, in the first approximation, produce a significant effect altering the constant of rigidity of the cantilever which acquires a new effective value $k_{eff} = k + \sigma$, where σ is the sum of the force derivatives for all the forces F_i affecting the cantilever

$$\sigma = \sum_i \partial F_i / \partial z \ . \quad (2)$$

Here z is the displacement of the tip relative to the specimen. Considering that $k = m\omega_0^2$, the phase angle ϕ_0 for oscillations at the resonance frequency ω_0 [4] is determined by the expression

$$\phi_0 = \tan^{-1} \left(\frac{k}{Q\sigma} \right). \quad (3)$$

Then the shift of the angle of the phase $\Delta\phi_0$ between the values for the free and contacting cantilever is determined as

$$\Delta\phi_0 \approx \frac{Q\sigma}{k}, \quad (4)$$

where σ is very small compared with k. The sign of the shift of the phase angle (phase shift below) coincides with the sign of the force derivative σ. Hence, the phase shift is positive when the full force acting upon the tip is repulsive and negative when the force induces attraction.

Numerical modeling of the dynamic AFM mode has been reported in [4]. The Van-der-Waals potential has been used to describe the forces of attraction and the elastic response of the material at indentation has been used to describe the forces of repulsion. It is demonstrated that the rigidity of the tip and the specimen is significant for determination of the magnitude and the duration of the effect of the force of repulsion in the tip-specimen system and the depth of indentation into the specimen. Elastic deformation due to the contact loading upon the specimen may be estimated in accordance with the Hertzian theory. Assuming that a spherical indenter (tip) with the radius of interactions R and a flat surface under the effect of force F produce a round contact spot with the radius a and the depth of penetration is d, the rigidity of the elastic contact couple S can be expressed as

$$S = \frac{\partial F}{\partial d} = \varepsilon a E^* , \quad (5)$$

where ε is a constant which depends on the shape of the indenter (ε = 2 for the sphere), E^* is the effective modulus of elasticity.

When the tip and the specimen come into contact, it is possible to approximate the full derivative of the force σ by the rigidity in the tip-specimen contact [4]. Determination of the rigidity from equation (5) is valid when the probe is in constant contact with the specimen surface. Only a momentary contact occurs in the intermittent mode during each oscillation cycle, the area of contact between the tip and the specimen changes in time during each contact cycle. Hence, the values of the contact radius a and rigidity S should be averaged in time within each single oscillation cycle. When the full derivative of the force is determined by the surface rigidity $\sigma \approx \langle S \rangle = \varepsilon \langle a \rangle E^*$, Eq. (4) is recorded as

$$\Delta\phi_0 \approx \varepsilon \langle a \rangle E^* \left(\frac{Q}{k} \right). \quad (6)$$

Equation (6) shows that the image of the phase shift presents the change in the rigidity of the surface layers of the material within the studied area. A more rigid area has a more positive phase shift, hence, it is more pronounced in the phase image. The rigidity is proportional to the reduced modulus of elasticity E^* which is determined by the Young modulus of the specimen's material, when the tip of the probe is much more rigid than the specimen. Hence, the image of the phase contrast provides a method of estimating the pattern of non-homogeneity and mapping surface properties of a material, namely the modulus of elasticity.

Results and Discussion. The structure of TiN coatings has been studied sufficiently enough. It had been earlier demonstrated that the structure of a TiN surface could be quite non-homogeneous with different zones [5]. The method of transmission electron microscopy and X-ray diffraction analysis corroborate that local regions of the material have different micro- and submicrostructures,

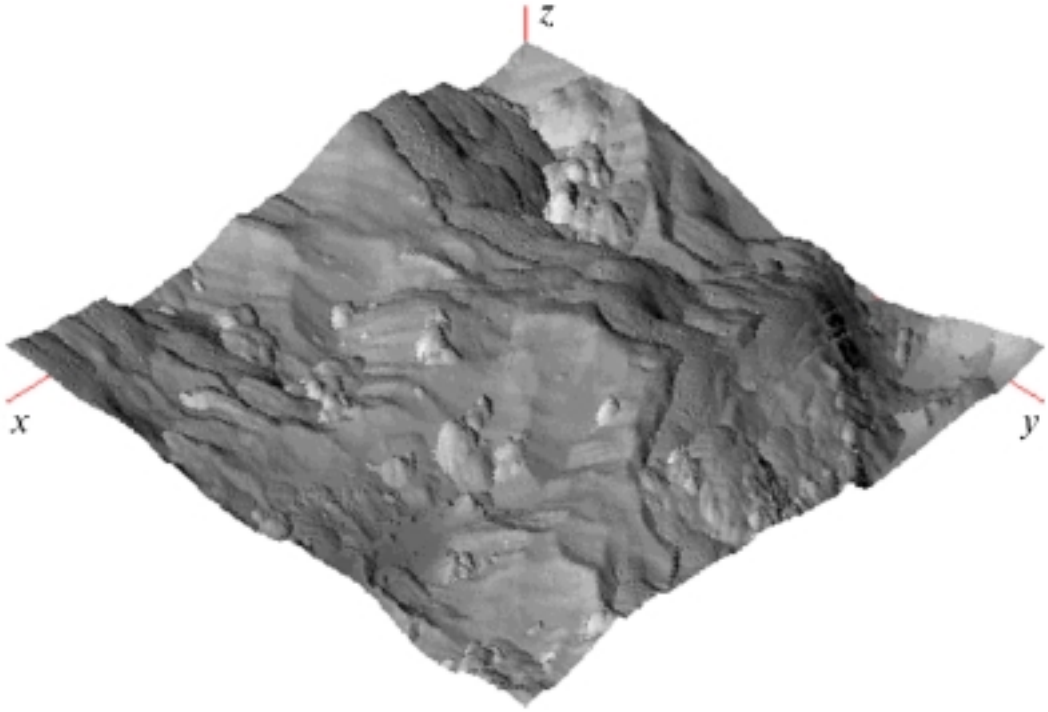

Fig. 3. Three-dimensional AFM-image of TiN coating microrelief. Scan size 9.7 μm, $Í_{max}$ = 438 nm, R_q = 79.2 nm

the processes of their formation are governed by the temperature of coating deposition, gas pressure in the process chamber and energy of bombarding ions.

Our AFM measurements have manifested that the TiN-coating surface has a developed topography featuring stepped projections (Fig. 3). The RMS deviation of the roughness R_q over the spots of scanning 10½10 μm amounts to 80—150 nm.

Examination of the phase contrast images can yield specific information. The images of the phase shift indicate a substantial local non-homogeneity of the micromechanical features of the coating. The surface layers represent alternating rigid and soft portions. A strong contrast between the regions with different properties gives grounds to assume that the coating consists of different phase structures. Phase of TiN is more rigid and the softer structure is formed by the by-products of the process of the coating deposition arranged predominantly over the grain boundaries. The specific share of the areas of lighter A_x and darker A_u sites in the area of scanning A_0 has been estimated, $A_u/A_0 \approx 0.15$ for the site 20½20 μm in area. Yet, zones with different structures (4—10 μm in area) can be identified within which these shares are quite different. Figure 4 shows the results of AFM measurements for the typical regions (zones) of the coating. The overwhelming area of the coating shows continuous (amorphous) sites which are very smooth (R_q = 7—9 nm) and very rigid (a slight phase shift $\Delta\phi_{max}$ =130°) (zone I). "Chip-shaped" rigid TiN portions alternate with softer interlayers, with the density of alternation of the rigid and soft material reaching high values within the individual regions (zone II). Apparently these regions form the grain boundaries with high roughness (R_q = 140 nm for the portion of the surface in Fig. 4, *c*). Moreover, portions are visible with a fine subgranular structure (zone III) which are quite smooth (R_q = 64 nm for the portion of the surface in Fig. 4, *e*) with thin boundaries between the grains of submicrometer size.

The roughness of the coating surface relates visibly to the pattern of the structures within a given portion. Yet, direct comparison of the images of the topography with the phase shift indicates that there is no regular correlation between the geometrical (topography) and material (phase contrast) structures. Softer zones may be located on the surface without adding to the roughness.

Thereafter the TiN coating friction surface was analyzed after 10^5 cycles of rolling by the steel roller. Comparison of the coating topography before and after friction has indicated the smoothing of the edges of the stepped structures (Fig. 5). The degree of roughness of the coating along the friction

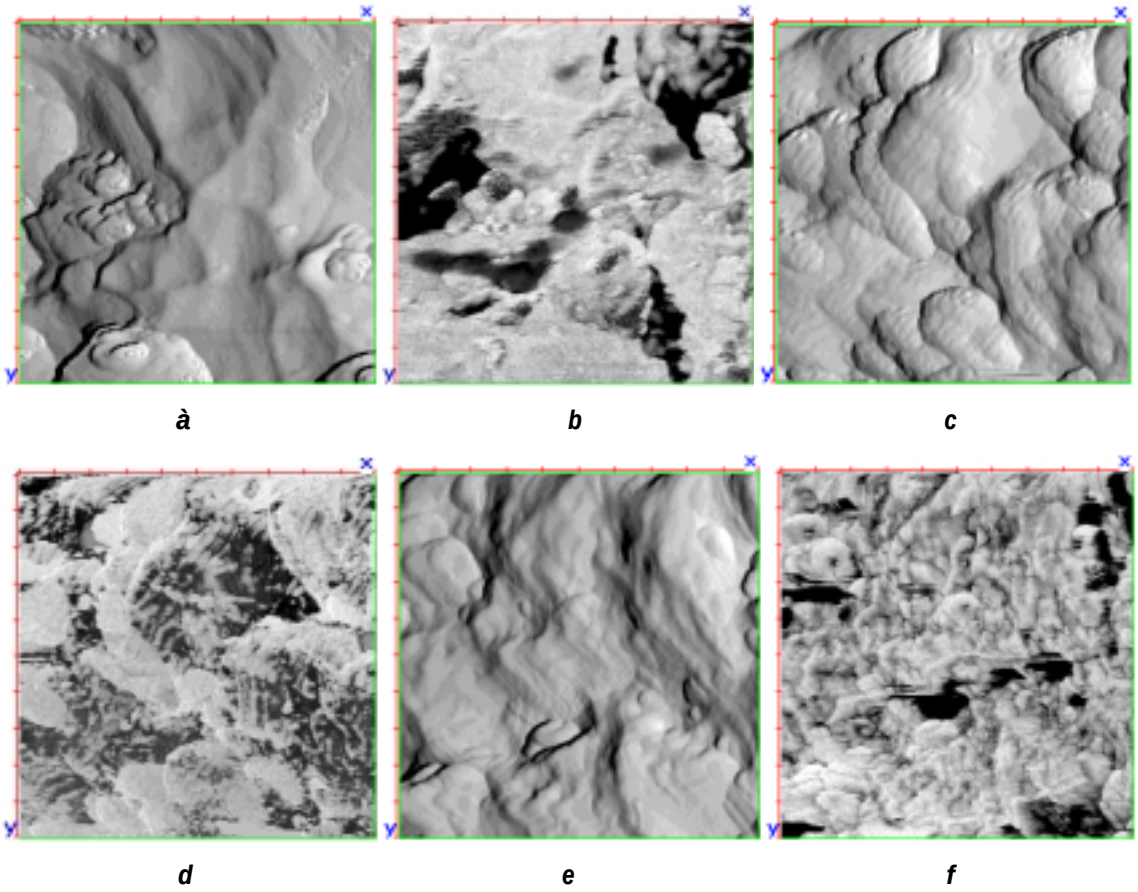

Fig. 4. AFM images of different TiN coating zones: *a, c, e* — topography; *b, d, e* — phase contrast. Zone I — *a, b* scan size 4.4 μm, H_{max} = 353 nm; $\Delta\phi_{max}$ = 130°, A_u/A_0 = 0.062. Zone II — c, d — scan size 8.7 μm, R_{max} = 816 nm; $\Delta\phi_{max}$ = 109°, A_u/A_0 = 0.250. Zone III — *e, f* — scan size — 8.8 μm, R_{max} = 360 nm; $\Delta\phi_{max}$ = 76°, A_u/A_0 = 0.074

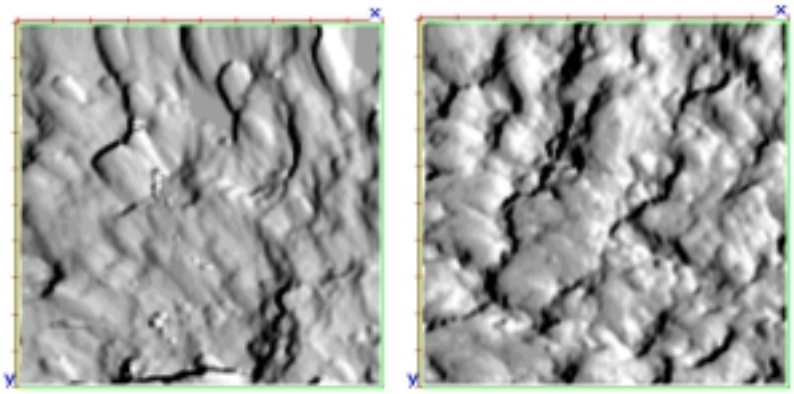

Fig. 5. Comparison of TiN topographies before (*a*) and after (*b*) friction: *a* — H_{max} = 757 nm, R_q = 107 nm; *b* — H_{max} = 530 nm, R_q = 89 nm; scan size 19.7 μm

path reduced approximately 1.5 times. Some fragmentation of the extended chip-shaped structures of the original coating is also visible.

Analysis of the phase contrast images yields more information showing three regions: white, black and intermediate gray (Fig. 6). Redistribution of the soft and rigid regions of the material in respect to the topographic sites of the friction surfaces is strongly different from the distribution of the rigidity of the material on the original TiN surfaces. Analysis of the pattern of this redistribution of

the material on the topographic structures can be useful for identifying the mechanism of origination of the layers with different rigidities on the friction surfaces. Representation of the scanning data in the form of a combined image integrating the images of topographies and phase contrasts (Fig. 6, *c*) turned out to be quite informative.

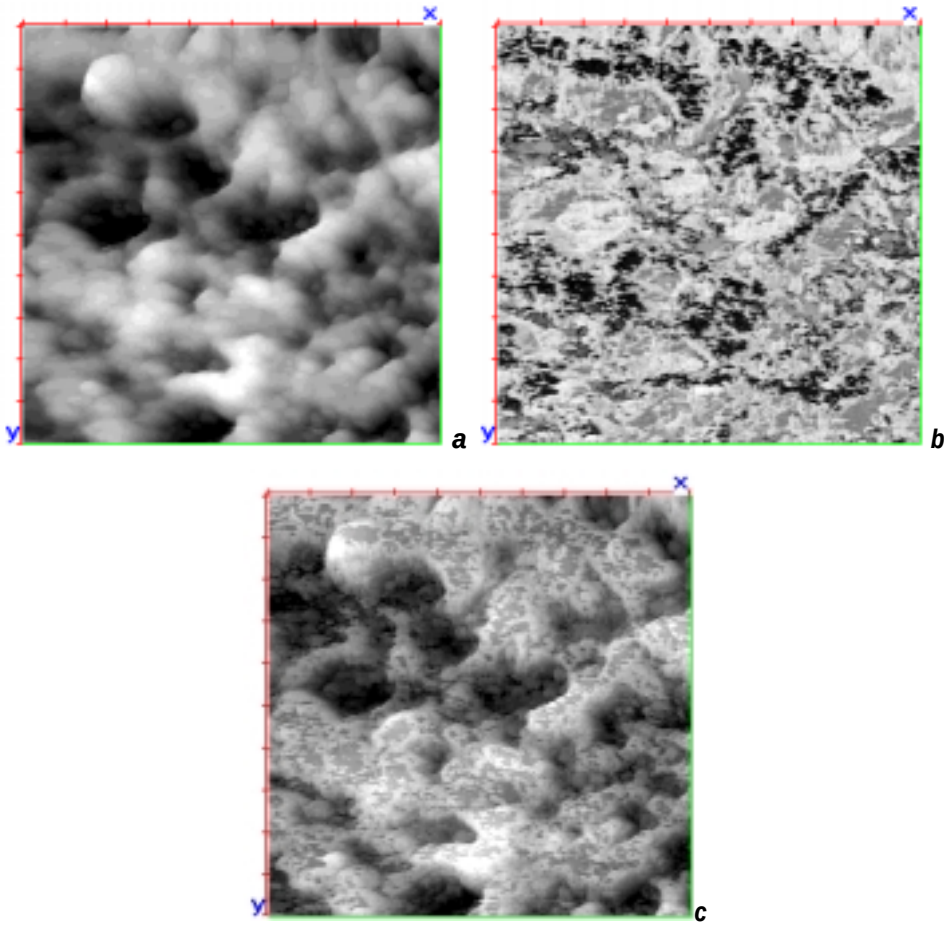

Fig. 6. Surface of TiN after rubbing against steel: *a* — topography; *b* — phase contrast image; *c* — combined image. After scanning 19×19 μm, H_{max} = 446 nm, $\Delta\phi_{max}$ = 140°, R_q = 83.2 nm

A visible separation of colors on the map of rigidity of the surface layers, which can be termed as the phase contrast image, proves that it is possible to attribute each color to a specific material. It is natural to assume that most rigid TiN portions correspond to the white color. Gray color may relate to the steel layers transferred plastically to the rigid TiN coating. Round-shaped particles accumulating in the valleys of the microrelief are colored gray (with a somewhat darker hue). It can be assumed that they are steel wear particles, which are rounded by rolling friction. Also, there are black-colored portions, which correspond to the material in the studied system with the least rigidity. It can be assumed that these portions correspond to the layers appearing in the friction zone due to tribochemical reactions.

Comparison of the AFM-measurements imaged as a three-dimensional surface structure with the planar distribution of the micromechanical features allows us to estimate the thickness and lateral dimensions of the layers appearing on the surface. Figure 7 shows the data of this analysis for various portions of the friction surface.

The profile of the largest particle in the field of scanning indicates that its lateral dimensions are about 1 μm and it is 57.3 nm thick (Fig. 7, *b*) evidencing a plate shape of the particle.

This type of particles may correspond to the fatigue mechanism of wear rather than to abrasion. Most of the particles registered over the analyzed portion have submicrometer lateral dimensions. The finest are about 100 nm in size. The particles are arranged in the space between the asperities and fill

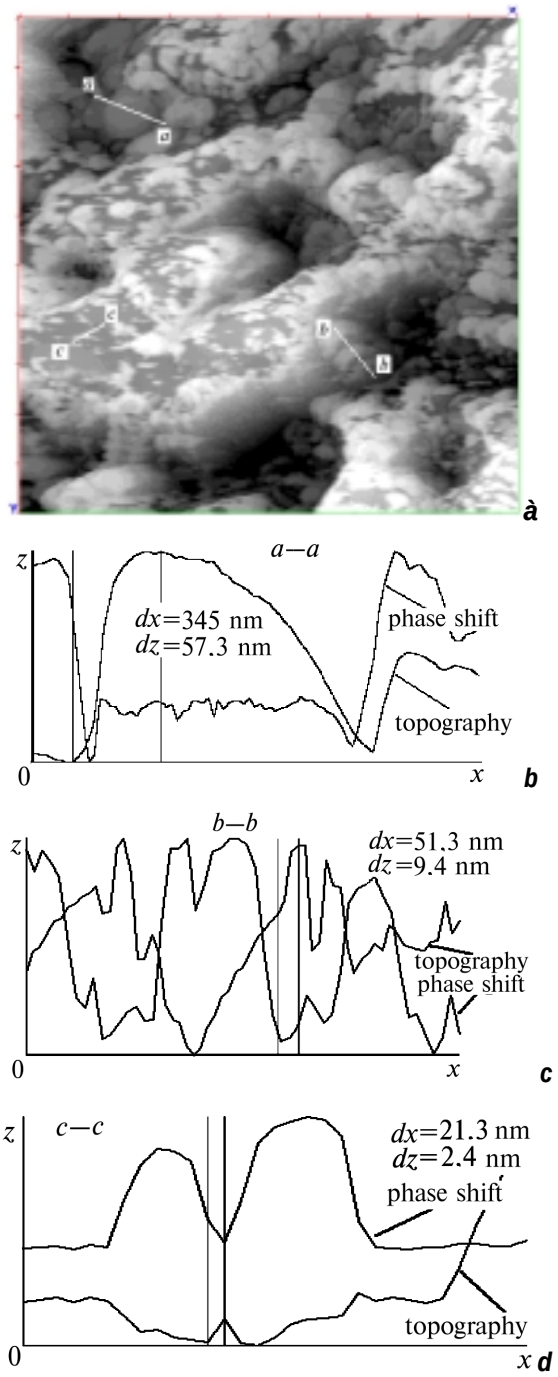

Fig. 7. Combined image of topography and phase shift for friction surface (arrow indicates friction direction) over portion 9×9 μm (*a*) and corresponding profile sections for topography and phase contrast images (*b*—*d*)

up the deepest valleys of microrelief. This factor of appearance of the "pockets" trapping free debris is positive as it reduces the abrasive effect of loose debris.

The material with a similar hue of the gray phase contrast is visible over the slopes of the microrelief, over its edges arranged in the direction of friction, which are most resistant to shear during microsliding and cutting of the softer material. Measurements of the thickness of the layers transferred by plastic smearing when steel adheres to the TiN surface, indicate that they are 9—15 nm thick (Fig. 7, *c*). Such transfer of fine layers from the surface of one rubbing body to the other may be attributed to the adhesive mechanism of wear of the metallic layers after their plastic deformation. This

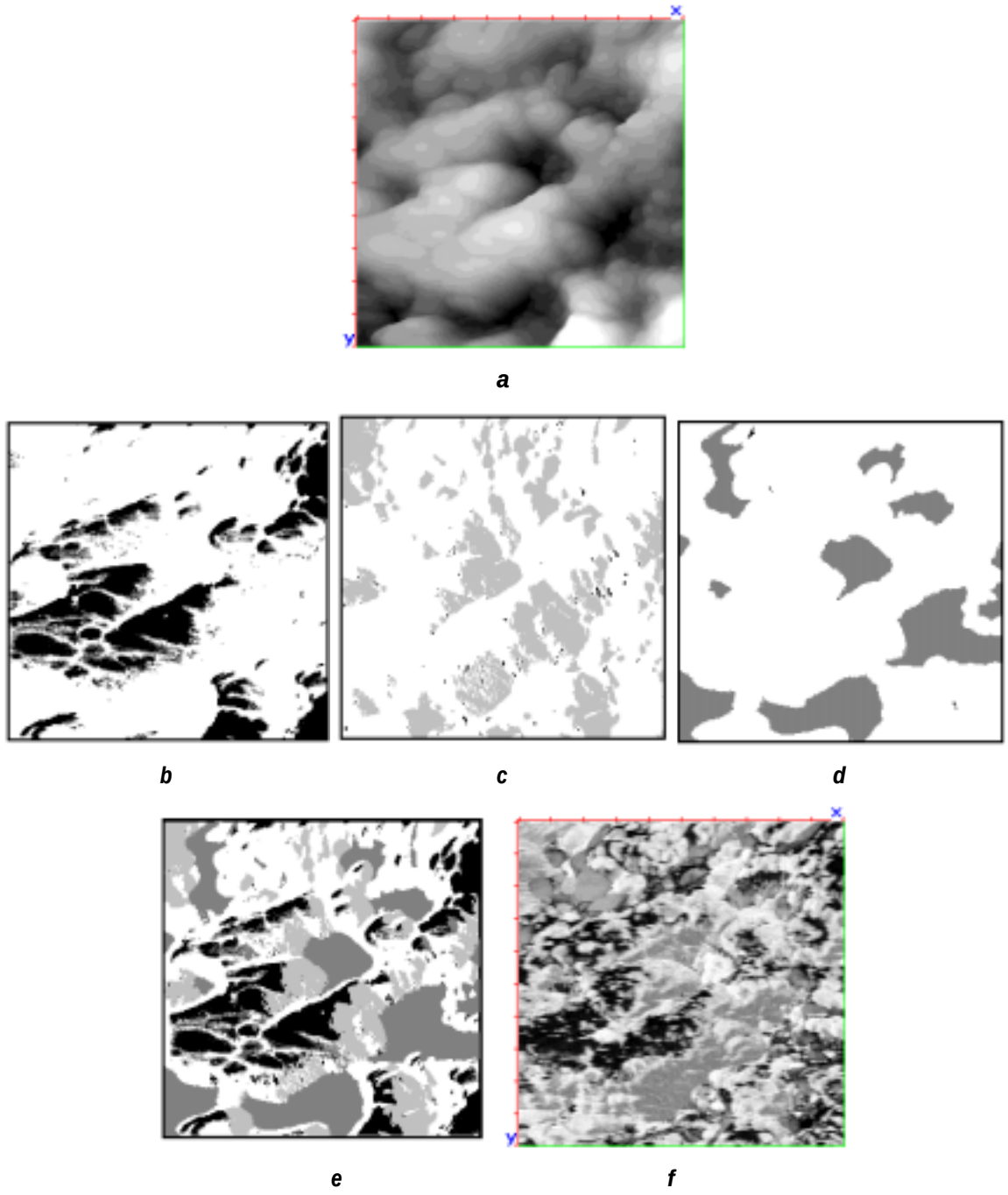

Fig. 8. Results of computer analysis and synthesis of friction surface: *a* — AFM-image of TiN friction surface topography (after scanning 9.5×9.5 μm, H_{max} = 351 nm, R_q = 67.2 nm); *b* — epure of contact pressure over the same surface portion; *c* — edges of microrelief exposed to shear stress at sliding; *d* — deepest microrelief depressions; e — synthesized friction surface; *f* — phase-contrast AFM-image ($\Delta\phi_{max}$ = 137°)

pattern of wear is observed in the zones where maximum shear stresses are effective due to the relief features of the more rigid friction surface.

The regions of the softest material (black color) are arranged over the tops of asperities dominating in the analyzed portion. The maximum contact pressures occur exactly over these areas (real contact spots) with the resulting maximum heat generation at friction. It is natural to assume that the appearance of the soft layers in the real contact zone between rough surfaces is due to the tribochemical processes evolving at the contact spots. Local discontinuity of the appearing films is a typi-

cal feature, with the hard TiN coating exposed in the discontinuities. Measurement of the film thickness in one such discontinuity has shown that it equals 2.4 nm (Fig. 7, *d*). Evaluation of the thickness of the soft layers in various points of the surface has manifested that this value ranges within 2—5 nm. It corresponds to the pattern of boundary molecularly fine layers of tribochemical transfer. Their origination is due to the chemical mechanism of wear evolving in the TiN-steel contact. Regretfully, the methods of studies used here have not allowed us to determine the chemical composition of the tribochemical layers appearing locally. It is a rather intricate task to be investigated independently.

Determination of the areas of the TiN friction surface, transferred steel, including debris, and tribochemical layers for the friction surface shown in Fig. 7 gave the following percentages: 51.4%, 34.8% and 13.8%. It is apparent that the transfer of steel to the TiN surface may have a dominating character in wear of the TiN-steel friction couple.

From the above assumptions about the nature of the surface layers with strongly different rigidities appearing on the TiN friction surface it has been attempted to perform computer modeling of a portion of the friction surface. The microtopography of the portion analyzed above (Fig. 8, *a*) was chosen for the study. The relief of the surface provided the original data for modeling.

First, the actual contact area was modeled using the algorithm described in [6]. Figure 8, b shows the image of contact spots and distribution of contact pressure over them, which resulted from calculations. It is noteworthy that there is a sufficiently good correlation between the contact area and the region of the soft material on the image of the phase contrast (Fig. 8, *f*) which are, according to our assumptions, layers of tribochemical origin.

Second, computer "illumination" has revealed the edges of the relief oriented in the direction of friction (Fig. 8, *c*). Exactly these edges may obstruct sliding and induce shear stresses in the soft material accompanied by the transfer of material from the steel indenter.

Third, the deepest depressions have been identified in which debris accumulate (Fig. 8, *d*).

Summation of the zones yielded by the computer modeling (Fig. 8, *b, c, d*) allows us to build a pseudo-image of the phase contrast (Fig. 8, *e*). The white color in this image corresponds to the TiN portions uncovered by debris. Comparison of the model image with the AFM-image of the phase contrast (Fig. 8, *f*) shows a certain correlation between the calculated and experimental results. It confirms that our assumptions about the origination of layers with different rigidities on the friction surface are not contradictory. More substantial discrepancies for the zones of steel transfer and accumulation of debris may be due to the fact that the original image chosen for modeling was the image of the surface already modified by friction, specifically so by the transfer of steel layers and accumulation of debris. Possibly the proportions of the areas of the calculated zones differ from the experimental one due to the same reason, namely 40.5%, 44.9%, 44.6% for TiN materials, transferred steel, and tribochemical layers, respectively. The calculated estimates have also shown the largest role of steel debris transfer to the TiN surface in the process of wear of the TiN-steel friction couple.

Conclusions. So, the effectiveness of the methods has been demonstrated based on the atomic force microscopy for investigating friction surfaces, detection and imaging of the layers of friction transfer, evaluation of their non-homogeneity and thickness. Combined analysis of the images of the topography and the surface phase contrast yields more comprehensive information.

Combined effect of different mechanisms of wear in the TiN-steel system has been demonstrated. These mechanisms include tribochemical wear accompanied by the appearance of fine boundary layers, adhesive wear, and fatigue wear of steel, as well as wear of TiN smoothing the edges of the TiN microrelief. Adhesive transfer of steel to the TiN surface and fatigue wear of steel with the appearance of debris can be assumed to be dominating in the TiN-steel friction couple.

Notwithstanding the mapping of the rigidity, the accomplished analysis is considered incomplete, since it does not yield any quantitative assessments of the micromechanical features of surface layers. Further progress of AFM methods in this direction is real and it can be based on nanoindentation and force spectroscopy. Yet, harder probe tips, such as diamonds, are needed to investigate harder materials.

REFERENCES

[1] Y.L. Su, J.S. Lin, L.I. Shiau, and J.D. Wu, *Wear*, vol. 167, pp. 73—83, 1993.
[2] S.A. Chizhik, V.V. Gorbunov, and A.M. Dubravin, *Proc. of the Conf. Computer Methods and Inverse Problems in Non-Destructive Testing and Diagnosis*, p. 33, Minsk, 1995.
[3] S.N. Magonov, V. Eling, and M.-N. Whango, *Surf. Sci.*, vol. 375, L385, 1997.

[4] D. Sarid, *Scanning Force Microscopy with Application to Electric, Magnetic and Atomic Forces*, New-York & Oxford, 1991.
[5] V. Valvoda, *Surf. and Coat. Technol*., vol. 80, pp. 61—65, 1996.
[6] S.A. Chizhik, V.V. Gorbunov, and N.K. Myshkin, Journal of Friction and Wear, Vol. 14, pp. 5—12, 1993.5

October 1999 Korea Institute of Science and Technology, Seoul,
V.A. Belyi Metal-Polymer Research Institute of Belarus National Academy of Sciences, Gomel